Electronic Supplementary Material (ESI) for Physical Chemistry Chemical Physics.

Supporting Information

Engineering Supramolecular Helical Assemblies via Interplay between Carbon(sp) Tetrel and Halogen Bonding Interactions

Burcu Dedeoglu, [a] Ayşe Gül Gürek,[a] Yunus Zorlu,[a]* Mehmet Menaf Ayhan [a]*

[a] Department of Chemistry, Gebze Technical University, Gebze, Kocaeli, Turkey

* Author for correspondence: menafayhan@gtu.edu.tr, yzorlu@gtu.edu.tr,

Materials and Methods

All chemicals and solvents were purchased from Sigma Aldrich and TCI Chemicals used as supplied without further purification unless stated otherwise. NMR spectra were recorded on a Bruker 400 spectrometer (^{1}H, 500 MHz; ^{13}C, 125 MHz). MALDI-TOF was performed on a Bruker Microflex LT MALDI-TOF-MS Instrument. Fourier-Transform Infrared (FTIR) spectra was recorded by Perkin Elmer Spectrum 100 Optical FT-IR Spectrometer.

The general synthesis of brominated phthalonitrile derivatives (1a-c)[1–3]

The corresponding methylphthalonitrile (1eq), NBS (10 eq) and benzoyl peroxide (ca. 0,2 eq) were mixed in carbon tetrachloride (40 ml) and the mixture was stirred vigorously and heated under reflux for 6 h. The solution was cooled to room temperature then filtered and the filtrate was evaporated to dryness. The products were purified by column chromatography on silica gel using a mixture of CH_2Cl_2:n-hexane (2:5, v/v) as eluent. The products fractions were collected and evaporated under reduced pressure to afford white solids.

4,6-Bis(dibromomethyl)isophthalonitrile (1a)

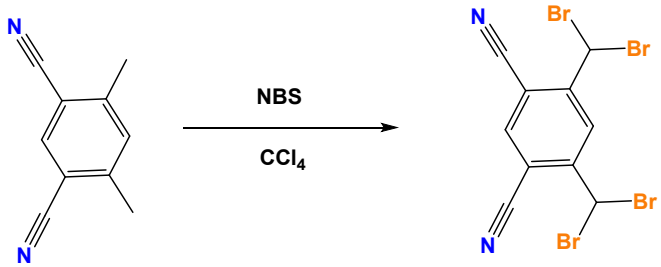

1a

Yield: 0,3 g (25 %). ^{1}H NMR ($CDCl_3$, 500 MHz) δ_H (ppm) = 6,96 (s, 2H), 7,91(s, 1H), 8,64 (s, 1H). ^{13}C NMR ($CDCl_3$, 500 MHz) δ_C (ppm) = 32.33, 110.7, 113.3, 131.5, 136.2, 149.2. IR (ATR) ν_{max} (neat)/cm^{-1} :2229 (CN). MALDI-MS (DHB) m/z: 471 $[M]^+$

4,5-Bis(dibromomethyl)phthalonitrile (1b)

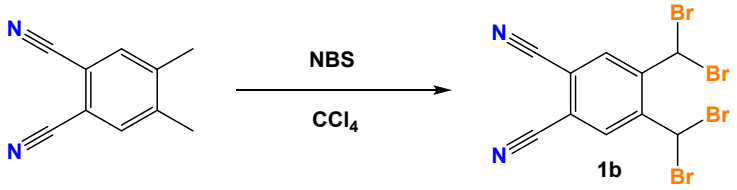

Yield: 0,6 g (20%). ^{1}H NMR ($CDCl_3$, 500 MHz) δ_H (ppm) = 7.0 (s, 2H), 8,2 (s, 2H). ^{13}C NMR ($CDCl_3$, 500 MHz) δ_C (ppm) = 32,2, 113.9, 117.2, 134.6, 142.1. IR (ATR) ν_{max} (neat)/cm^{-1}: 2237 (CN). MALDI-MS (DHB) m/z: 471 $[M]^+$

2,5-Bis(bromomethyl)terephthalonitrile (1c)

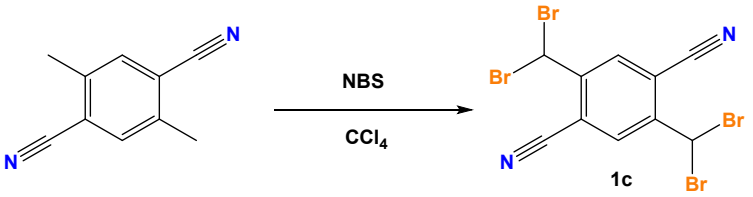

Yield: 0,4g (21%). ^{1}H NMR ($CDCl_3$, 500 MHz) δ_H (ppm) = 6,94 (s, 2H), 8,28(s, 2H). ^{13}C NMR ($CDCl_3$, 500 MHz) δ_C (ppm) = 32.5, 109.9, 113.6, 139.9, 145.2. IR (ATR) ν_{max} (neat)/cm^{-1}: 2237 (CN). MALDI-MS (DHB) m/z: 471 $[M]^+$

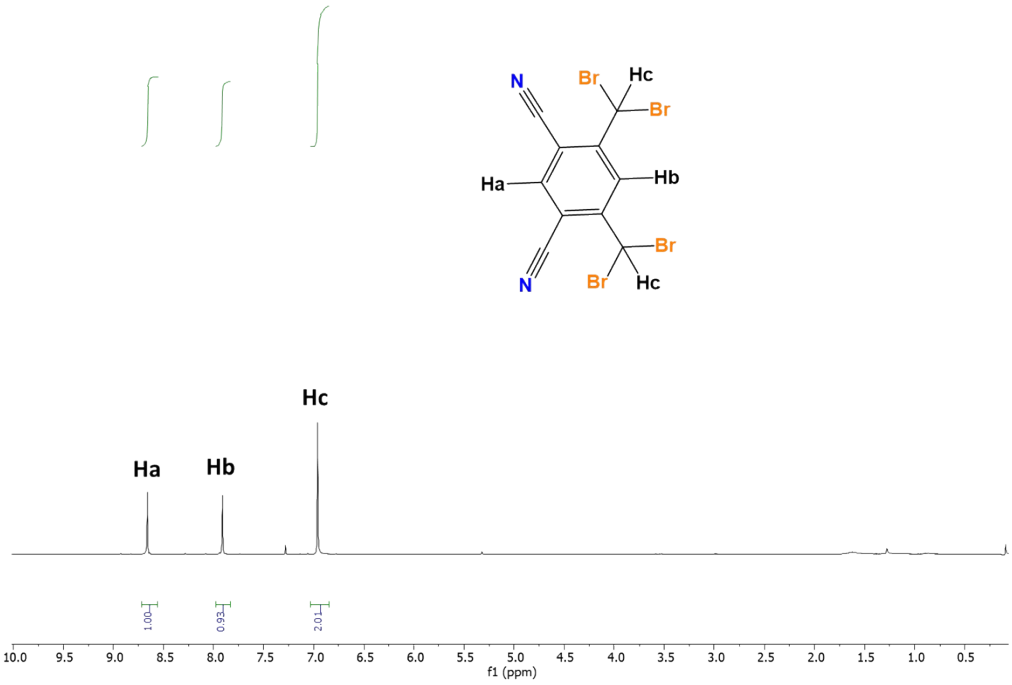

Figure S1: ^{1}H NMR Spectrum of the Compound **1a** in $CDCl_3$

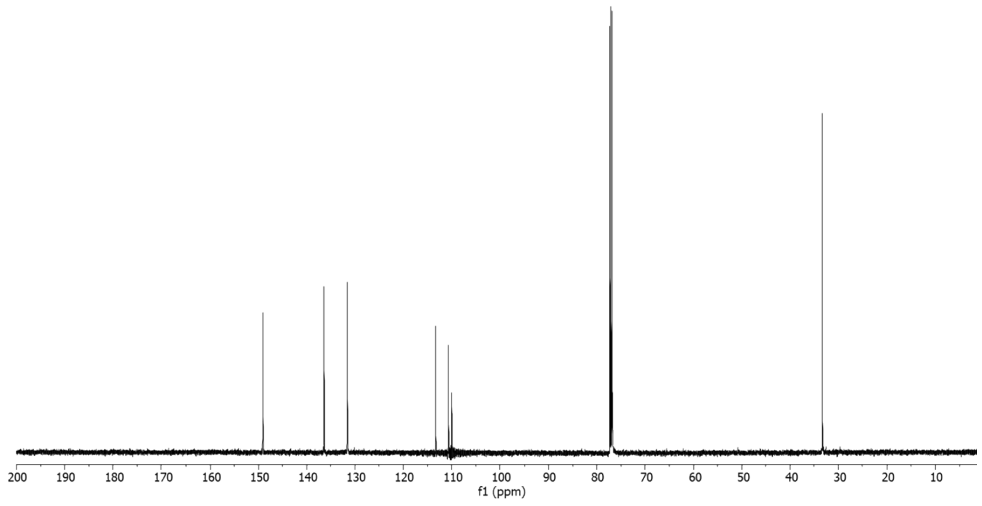

Figure S2: ^{13}C NMR Spectrum of the Compound **1a** in $CDCl_3$

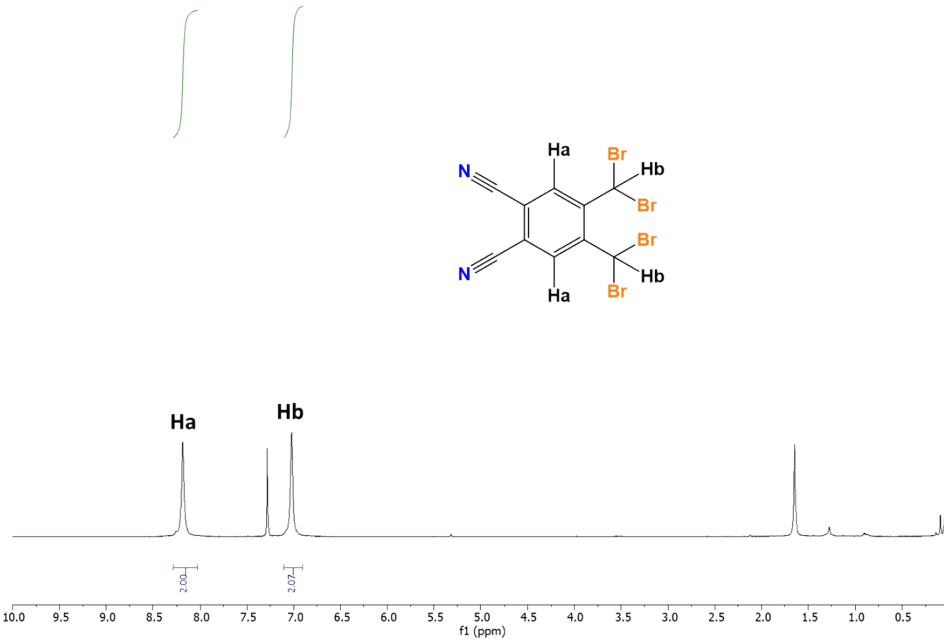

Figure S3: ^{1}H NMR Spectrum of the Compound **1b** in $CDCl_3$

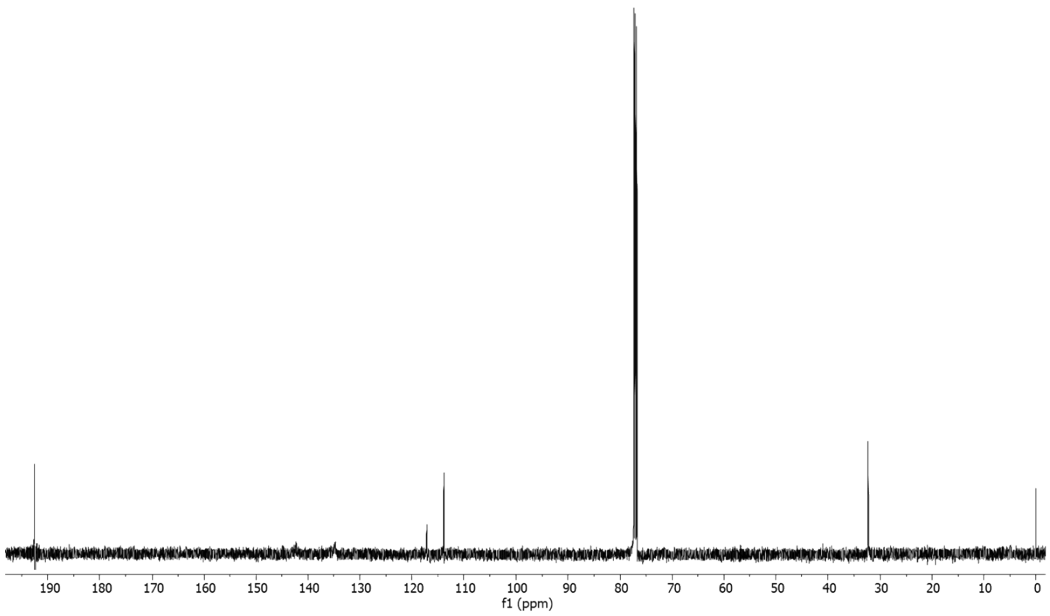

Figure S4: ^{13}C NMR Spectrum of the Compound **1b** in $CDCl_3$

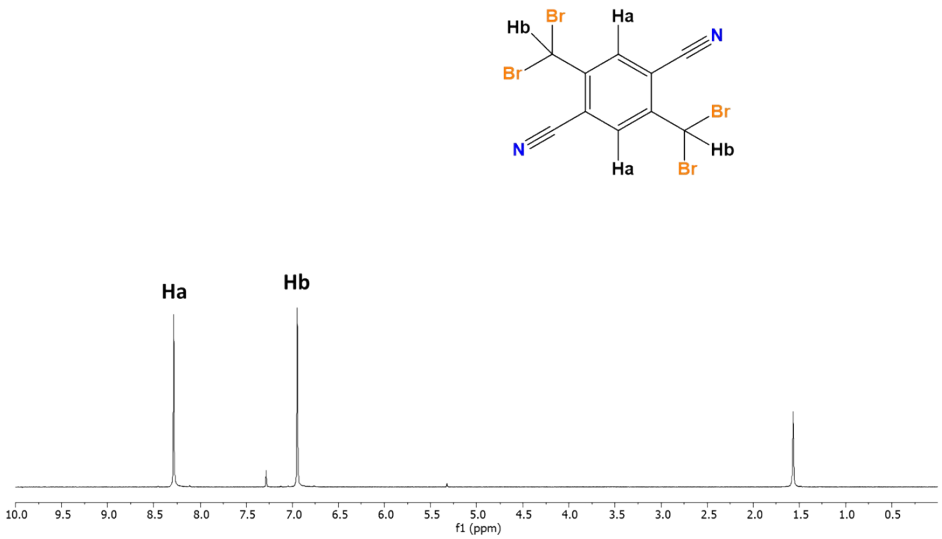

Figure S5: ^{1}H NMR Spectrum of the Compound **1c** in $CDCl_3$

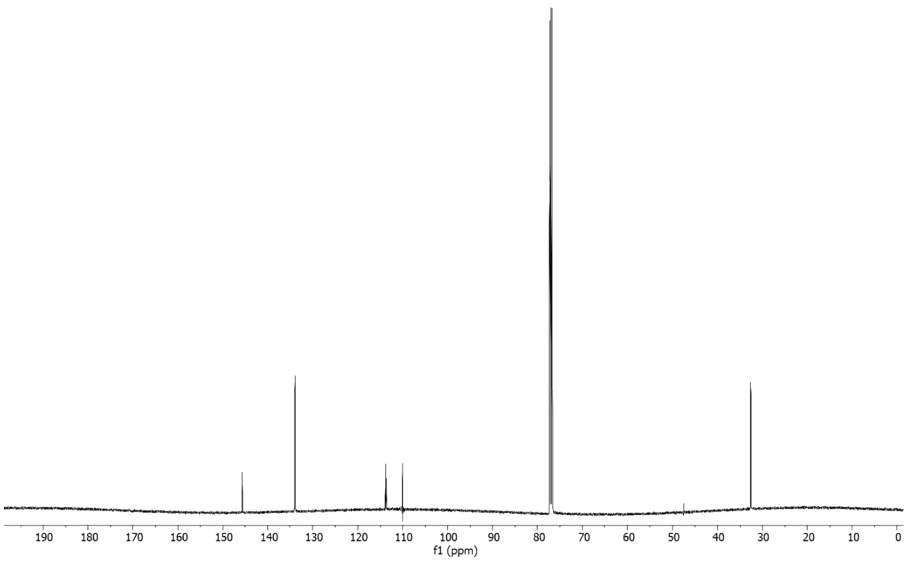

Figure S6: ^{13}C NMR Spectrum of the Compound **1c** in $CDCl_3$

X-Ray Data Collection and Structure Refinement

Data were obtained with Bruker APEX II QUAZAR three-circle diffractometer. Indexing was performed using APEX2.[4] Data integration and reduction were carried out with SAINT.[5] Absorption correction was performed by multi-scan method implemented in SADABS. [6] The structure was solved using SHELXT and then refined by full-matrix least-squares refinements on F^2 using the SHELXL. [7,8] Aromatic C-bound H atoms were positioned geometrically and refined using a riding mode. Crystallographic data and refinement details of the data collection for compounds **1a-1c** are given in Table S1. Additional crystallographic data with CCDC reference numbers 1852924 (**1a**), 1852922 (**1b**), and 1852923 (**1c**) have been deposited within the Cambridge Crystallographic Data Center *via* www.ccdc.cam.ac.uk/deposit.

Table S1. Crystal data and structure refinement for **1a-1c**.

Identification code	1a	1b	1c
CCDC	1852924	1852922	1852923
Empirical formula	$C_{10}H_4Br_4N_2$	$C_{10}H_4Br_4N_2$	$C_{10}H_4Br_4N_2$
Formula weight	471.79	471.79	471.79
Temperature/K	296.(2)	176.(2)	296.(2)
Crystal system	monoclinic	monoclinic	monoclinic
Space group	$P2_1/n$	$P2_1$	$P2_1/c$
a/Å	9.7944(13)	7.9676(7)	6.2037(7)
b/Å	9.9395(12)	8.5676(7)	6.6476(8)
c/Å	13.1845(19)	9.6639(8)	15.677(2)
α/°	90	90	90
β/°	97.554(9)	105.119(5)	95.856(9)
γ/°	90	90	90
Volume/Å^3	1272.4(3)	636.85(9)	643.14(15)
Z	4	2	2
ρ_{calc}g/cm^3	2.463	2.460	2.436
μ/mm^{-1}	12.624	12.611	12.487
F(000)	872.0	436.0	436.0
Crystal size/mm^3	0.284 × 0.194 × 0.128	0.25 × 0.22 × 0.18	0.306 × 0.177 × 0.142
Radiation	MoKα (λ = 0.71073)	MoKα (λ = 0.71073)	MoKα (λ = 0.71073)
2Θ range for data collection/°	4.88 to 50.04	6.46 to 50	5.22 to 50.06
Index ranges	$-11 \le h \le 11$, $-10 \le k \le 11$, $-13 \le l \le 15$	$-9 \le h \le 9$, $-9 \le k \le 10$, $-11 \le l \le 11$	$-6 \le h \le 7$, $-7 \le k \le 7$, $-15 \le l \le 18$
Reflections collected	5476	7210	3469
Independent reflections	2248 [R_{int} = 0.0576, R_{sigma} = 0.0937]	2232 [R_{int} = 0.0548, R_{sigma} = 0.0628]	1107 [R_{int} = 0.0292, R_{sigma} = 0.0301]
Data/restraints/parameters	2248/0/145	2232/1/145	1107/0/73
Goodness-of-fit on F^2	1.041	1.055	1.095
Final R indexes [I>=2σ (I)]	R_1 = 0.0499, wR_2 = 0.1194	R_1 = 0.0407, wR_2 = 0.0970	R_1 = 0.0294, wR_2 = 0.0669
Final R indexes [all data]	R_1 = 0.0806, wR_2 = 0.1322	R_1 = 0.0513, wR_2 = 0.1011	R_1 = 0.0370, wR_2 = 0.0696
Largest diff. peak/hole / e Å^{-3}	0.73/-0.81	1.12/-0.61	0.76/-0.53

Hirshfeld Surface Analysis

In order to gain a better understanding of the intermolecular interactions **1a-1c**, Crystal Explorer program was used to generate Hirshfeld surfaces incorporating two-dimensional (2D) fingerprint plots.[9–11] The normalized contact distance (d_{norm}) surface, which expressed in terms of distances to the surface from the nuclei inside and outside the Hirshfeld surface (d_i, and d_e, respectively) and the vdW radii of the atoms (r_i^{vdw} and r_e^{vdw}), defined as Eq. 1 gives identification of the regions of particular importance to intermolecular interactions .[12,13] The 2D fingerprint plots (Fig S7, S8, S9), which were derived from the combination of d_i, and d_e, were used for quantifying the intermolecular contacts in the crystal.

$$d_{norm} = \frac{d_i - r_i^{vdw}}{r_i^{vdw}} + \frac{d_e - r_e^{vdw}}{r_e^{vdw}} \qquad \text{Equation } \mathbf{(1)}$$

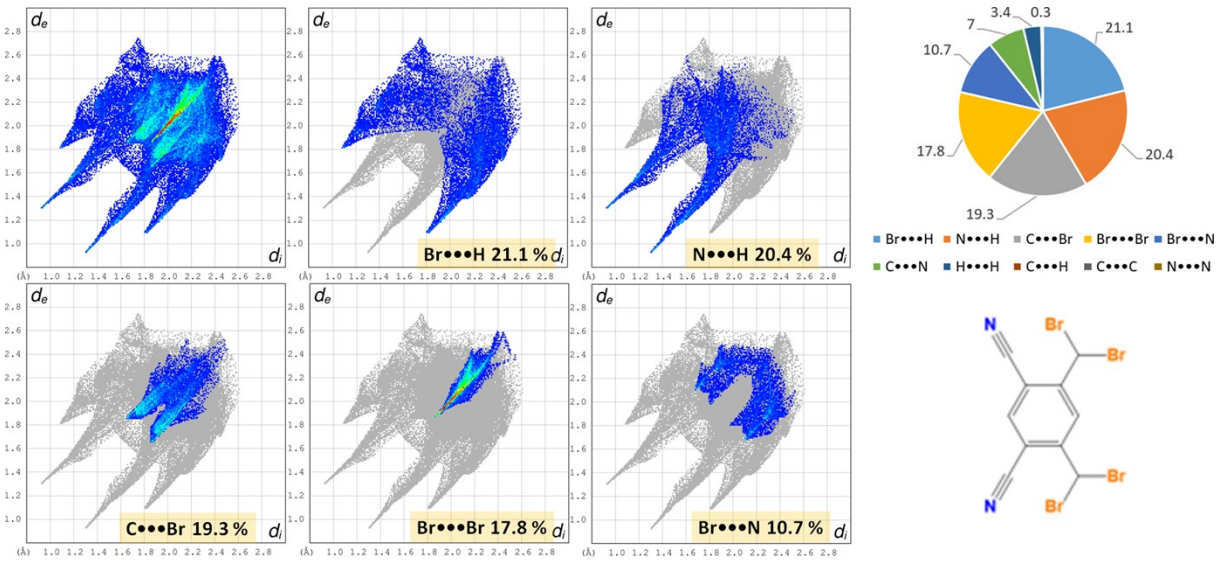

Fig. S7. The 2D fingerprint plots of **1a**, showing the percentage contributions to the total Hirshfeld surface area.

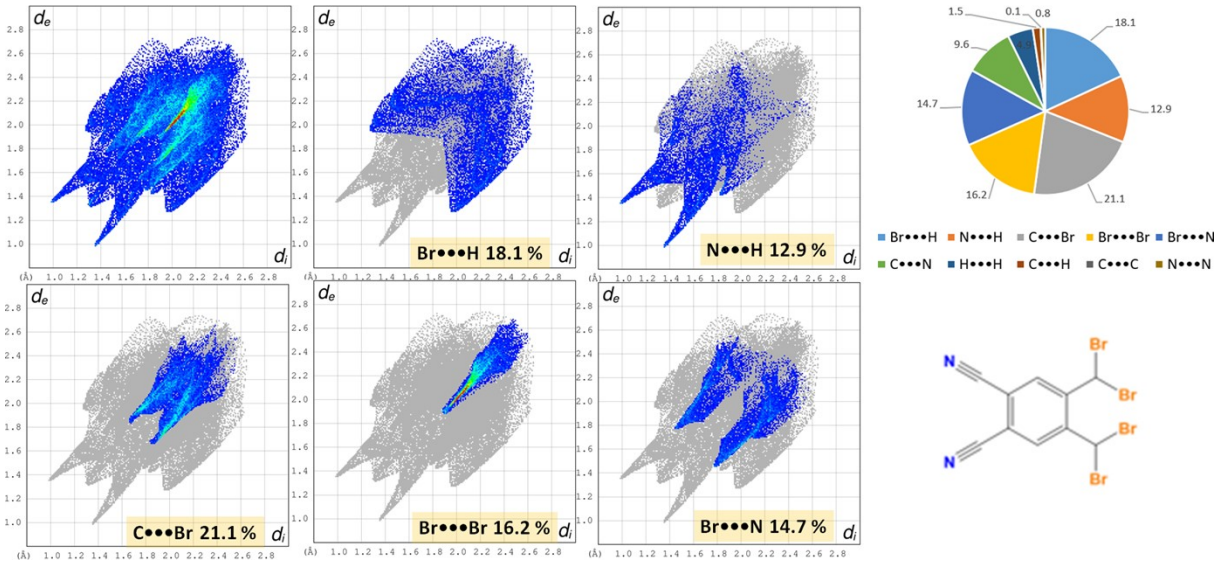

Fig. S8. The 2D fingerprint plots of **1b**, showing the percentage contributions to the total Hirshfeld surface area.

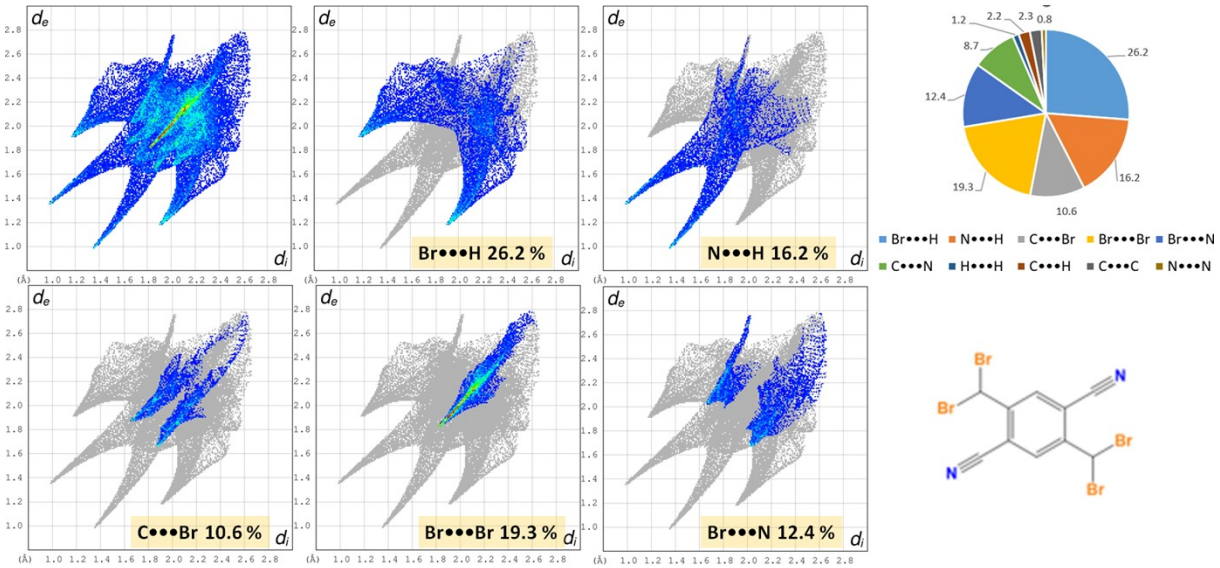

Fig. S9. The 2D fingerprint plots of **1c**, showing the percentage contributions to the total Hirshfeld surface area.

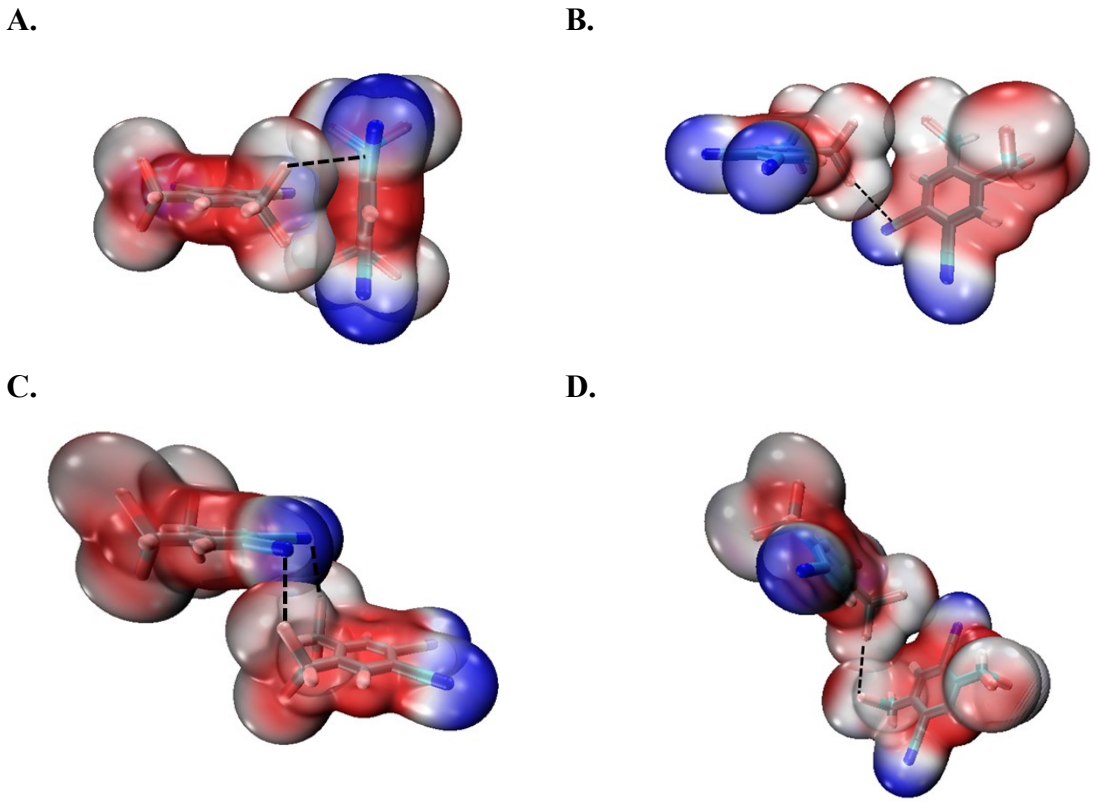

Fig. S10. Illustration of electrostatic complementary interactions and penetration of van der Waals surface in the dimers.

Table S2. Electron density (ρ,au), Laplacian ($\Delta^2\rho$, au) and energy density (H, au) at the intermolecular bond critical points in the dimers

	Interaction	***ρ *100***	**$\nabla^2\rho$*10**	***H*1000***
1a	Br··· Br	0.439	0.135	0.765
	Br··· CN	0.587	0.195	1.005
	Br··· NC	0.320	0.0997	0.521
	CN···C_{phenyl}	0.347	0.0989	0.413
	Br···C_{phenyl}	0.613	0.183	0.856
	Br··· Br	0.342	0.106	0.652
1b-I	Br··· Br	0.478	0.1526	0.843
	Br··· NC	0.622	0.202	0.880
Ib-II	Br··· NC	0.685	0.223	0.895
	Br··· πCN	0.239	0.0722	0.431
	Br··· NC	0.852	0.277	1.041
1c	Br··· NC	0.362	0.117	0.577
	Br··· H_{phenyl}	0.380	0.131	0.860
	Br··· Br	0.684	0.221	0.104
	Br··· Br	0.325	0.0996	0.616

Table S3. E2 Delocalization Energies Based on NBO Analysis.

Compound	Donor-Acceptor	E2 energy (kcal mol^{-1})
1a	LP(Br23) → σ*(C5-N19)	0.36
1b-I	π(C6-N20)→ σ*(Br24-C37)	0.62
1b-II	LP(N20) → σ*(Br23-C37)	0.39
1c	LP(Br31) → σ*(Br12-C18)	1.79

Table S4. Summary of SAPT results and interaction energies of the dimers.

Compound	E_{elst}	E_{exch}	E_{ind}	E_{disp}	E_{SAPT}	E_{int}
1a	-6.3	9.8	-1.4	-13.4	-11.4	-7.3
1b-I	-2.4	4.2	-0.6	-5.3	-4.0	-1.8
1b-II	-3.4	6.7	-1.1	-6.6	-4.4	-2.2
1c	-2.7	4.8	-0.7	-6.0	-4.6	-2.6

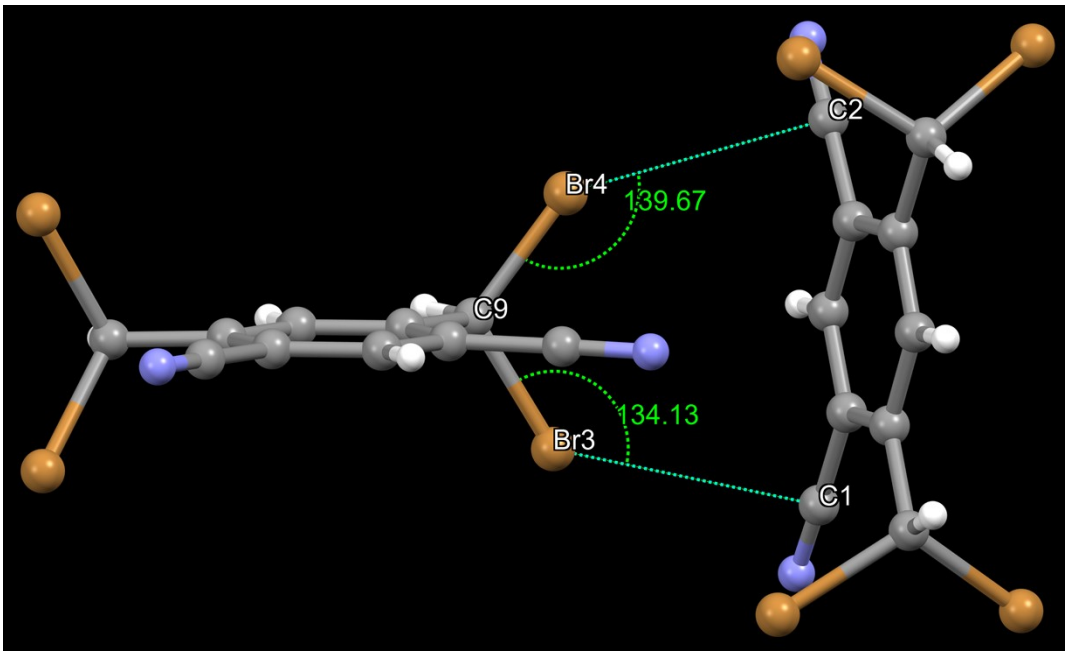

Fig. S11. The NC···Br tetrel bonding interactions showing C–Br···CN angle.

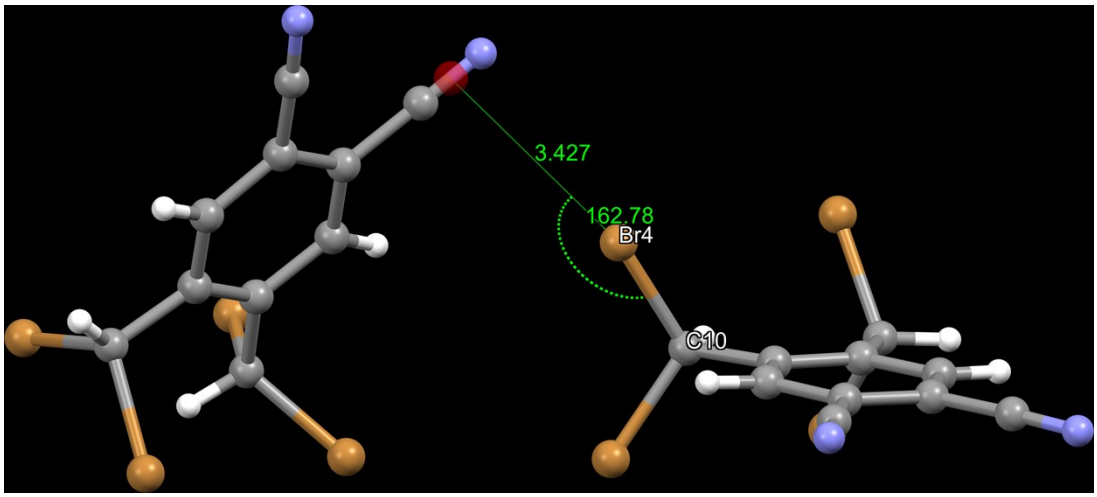

Fig. S12. The Br···π (-C≡N) halogen bonding interactions showing C–Br···π (-C≡N) angle.

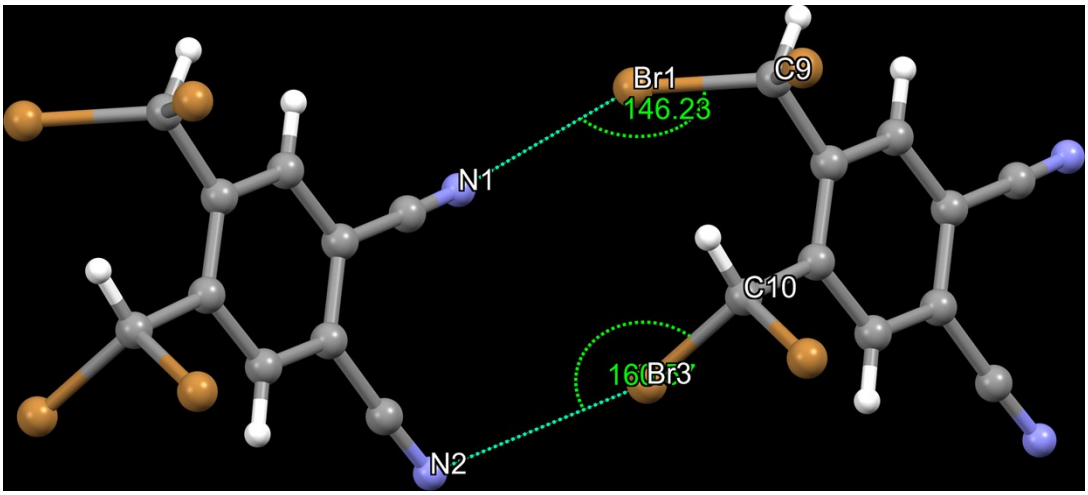

Fig. S13. The Br···N halogen bonding interactions showing C–Br···N angle.

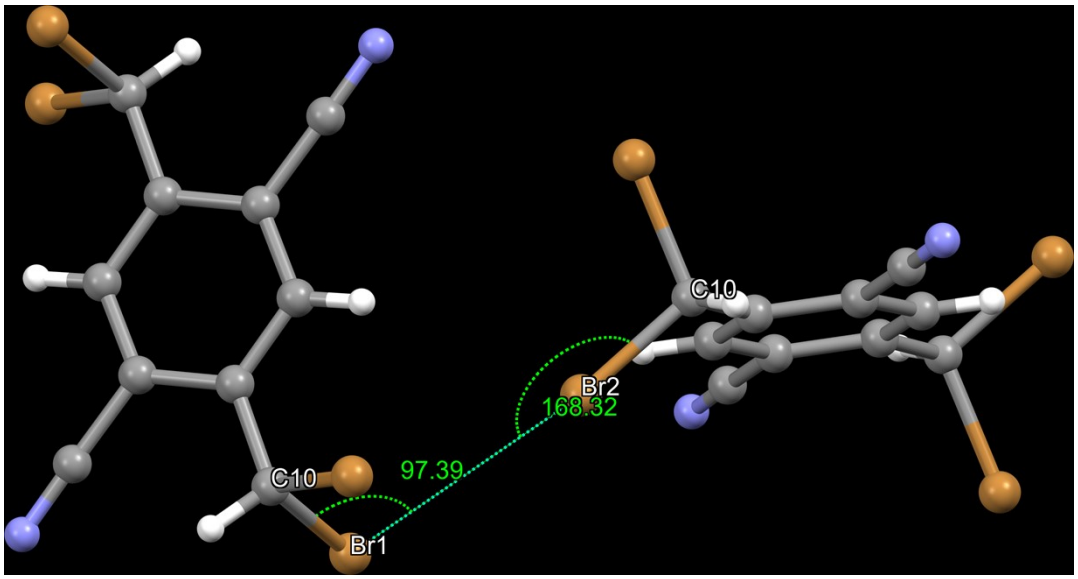

Fig. S14. The Br···Br type-II halogen bonding interactions showing C–Br···Br angles.

REFERENCES

1 C. M. A. Villalba, T. C. De Rozada, F. S. Dos Santos, L. Scorsin, J. R. Garcia and B. C. Fiorin, *Synth.*, 2018, **50**, 1259–1263.

2 J. Li, H. Lin, J. Huang and J. Yin, *Dye. Pigment.*, 2019, **170**, 107564.

3 R. F. Enes, J. J. Cid, A. Hausmann, O. Trukhina, A. Gouloumis, P. Vázquez, J. A. S. Cavaleiro, A. C. Tomé, D. M. Guldi and T. Torres, *Chem. - A Eur. J.*, 2012, **18**, 1727–1736.

4 APEX2. Ver. 2014.11-0, Bruker, 2014.

5 W. SAINT, version 8.34A, Bruker, Bruker AXS Inc., Madison, 2013.

6 W. SADABS, version2014/5, Bruker, Bruker AXS Inc., Madison, 2014.

7 G. M. Sheldrick, *Acta Crystallogr. Sect. C Struct. Chem.*, 2015, **71**, 3–8.

8 O. V. Dolomanov, L. J. Bourhis, R. J. Gildea, J. A. K. Howard and H. Puschmann, *J. Appl. Crystallogr.*, 2009, **42**, 339–341.

9 M. A. Spackman and D. Jayatilaka, *CrystEngComm*, 2009, **11**, 19–32.

10 M. J. Turner, J. J. McKinnon, S. K. Wolff, D. J. Grimwood, P. R. Spackman, D. Jayatilaka and M. A. Spackman, 2017.

11 M. A. Spackman and J. J. McKinnon, *CrystEngComm*, 2002, **4**, 378–392.

12 J. J. McKinnon, M. A. Spackman and A. S. Mitchell, *Novel tools for visualizing and exploring intermolecular interactions in molecular crystals*, 2004, vol. 60.

13 J. J. McKinnon, D. Jayatilaka and M. A. Spackman, *Chem. Commun.*, 2007, 3814–3816.